European Polymer Journal 45 (2009) 2450–2454

Contents lists available at ScienceDirect

European Polymer Journal

journal homepage: www.elsevier.com/locate/europolj

Interfacial change on morphological transitions in styrene–isoprene diblock copolymer

Jong-Eun Kim [a], Wang-Cheol Zin [a,*], Jong-Hyun Ahn [b,*]

[a] Department of Materials Science & Engineering, Pohang University of Science and Technology, Pohang 790-784, Republic of Korea
[b] School of Advanced Materials Science & Engineering, SKKU Advanced Institute of Nanotechnology, Sungkyunkwan University, Suwon 440-746, Republic of Korea

ARTICLE INFO

Article history:
Received 3 February 2009
Received in revised form 28 March 2009
Accepted 19 April 2009
Available online 3 May 2009

Keywords:
Block copolymer
Small-angle X-ray
Specific interfacial area
Order–order transition

ABSTRACT

The specific interfacial area (*S/V*) and interfacial thickness in each microstructure of styrene–isoprene diblock copolymer were estimated by analyzing the deviations from Porod's law. The thermally induced phase transitions proceeded from lamellae (L) to hexagonally ordered cylinder (HEX), *via* hexagonally perforated layer (HPL) and gyroid (G). The *S/V* ratio increased stepwise at the order–order transition (OOT) from L to HEX, *via* HPL and G. The *S/V* data can be utilized for OOT determination.

1. Introduction

Block copolymers composed of two or more chemically different polymer segments (or blocks) form a variety of ordered morphologies due to the energetic repulsion effects of the blocks [1–3]. By varying the composition of the block copolymer or the temperature, these structures can be controlled and various order–order transitions (OOTs) can occur. Earlier theories predicted only the classical morphologies, lamellae (L), hexagonally ordered cylinders (HEX) and spheres, to be stable. Recent experiments have observed additional complex bicontinuous structures such as hexagonally modulated layers (HML), hexagonally perforated layers (HPL), and the gyroid (G) by using small angle X-ray scattering (SAXS), small angle neutron scattering and transmission electron microscopy [4–15]. However, these investigations on bicontinuous phases required highly ordered structures made through especial sample preparation methods to observe the morphological transitions because of their weak diffraction patterns.

According to Porod's theory [16,17], the intensity in the tail of the SAXS curve of structures with sharp phase boundaries decreases in proportion to q^{-4}. Polymers often exhibit deviations from Porod's law, e.g., the product of $q^4 I(q)$ does not reach a constant value. Ruland showed a method for analyzing deviations from Porod's law using a model containing two phases connected by a transition layer [18]. By analyzing the deviation of the scattering curves at large q from Porod's law, the specific interfacial area (*S/V*) and interfacial thickness could be determined.

The present work focuses on the change of *S/V* in the styrene–isoprene diblock copolymer induced by morphological transitions. The OOTs obtained from the sharp change in *S/V* are compared with those determined by the change in diffraction patterns of SAXS and rheological measurements.

2. Theoretical background

In the case of an ideal, two-phase model having no measurable thickness, Porod's law is that $I(q)$ should decrease

* Corresponding authors. Tel.: +82 31 290 7400; fax: +82 31 290 7410.
E-mail addresses: wczin@postech.ac.kr (W.-C. Zin), ahnj@skku.edu (J.-H. Ahn).

0014-3057/$ - see front matter © 2009 Elsevier Ltd. All rights reserved.
doi:10.1016/j.eurpolymj.2009.04.025

as a function of q^{-4} for large q and that the proportionality constant should be related to the total area, S, of the boundaries between two phases in the scattering volume [16,17,19,20]

$$\lim_{q\to\infty}[I_{id}(q)] = \frac{2\pi(\Delta\rho)^2 S}{q^4} \quad (1)$$

where $\Delta\rho$ is the difference of electron density between the two phases. Any practical application requires the measurements of absolute intensity. In an idealized two-phase system, the invariant, Q_{th} is determined as [16]

$$Q_{th} = (\Delta\rho)^2\phi_1\phi_2 \quad (2)$$

where ϕ_1 and ϕ_2 indicate the volume fractions of the two phases, and the invariant, $Q_{\exp}$ can be evaluated by

$$Q_{\exp} = \frac{1}{2\pi^2}\int I(q)q^2\,dq \quad (3)$$

If the intensity is determined in relative units, the following Eq. (4) can be used to evaluate S/V.

$$\lim_{q\to\infty} I_{id}(q)q^4/Q = \frac{2\pi S}{\phi_1\phi_2 V} \quad (4)$$

Furthermore, in an idealized two-phase system, the Porod inhomogeneity length l_p is given by

$$l_p = 4\pi\phi_1\phi_2\frac{V}{S} \quad (5)$$

A two-phase system contains inhomogeneities within the individual phase, due to the atomic nature of the material and the density fluctuations at all size scales arising from thermal motions of atoms [18]. The scattered intensity arising from thermal fluctuation can be fitted empirically at relatively high q by [21–27]

$$I_B(q) = a + bq^n \quad (6)$$

where the arbitrary constants a, b and n (an even integer) have been found to fit the scattered curve at relatively high q. The fitted curve is then extrapolated to smaller values of q to be subtracted from the observed intensity.

The scattered intensity in the Porod region after removing the contributions due to the thermal density fluctuations within the phases can be applied to estimate the interfacial thickness, S/V, and invariant. In two-phase materials with diffuse boundaries, the equation is modified to [27–30,24]

$$I(q) = I_{id}(q)\exp(-\sigma^2q^2) \quad (7)$$

where σ is the standard deviation of the Gaussian smoothing function. In the plot of $\ln(q^4I(q))$ against q^2, the intercept, which is equal to $\ln\left(\frac{2\pi S}{\phi_1\phi_2 V}\right)$, and its slope, which is equal to $-\sigma^2$, can be obtained. In the case of a sigmoidal-gradient model, the interfacial thickness, t, can also be obtained from σ as follows [23,24,27–30]:

$$t = \sqrt{2\pi}\sigma \quad (8)$$

Due to the diffuse interface, the invariant can be reduced to [31]

$$Q = (\Delta\rho)^2\phi_1\phi_2\left(1 - \frac{t}{l_p}\right) \quad (9)$$

3. Experimental

3.1. Materials

A styrene–isoprene diblock copolymer (PSI0101) was synthesized by living anionic polymerization with sec-butyllithium as an initiator under cyclohexane at 45 °C. The number-averaged molecular weight, M_n, was 4.24×10^4, as determined by GPC, and the polydispersity index, M_w/M_n, was 1.03 with M_w being the weight-averaged molecular weight [32]. The volume fraction of PS determined by ^{1}H NMR was 0.333. The sample was prepared by solution casting in toluene (~10 wt.% solid) in the presence of an antioxidant (Irganox 1010, Ciba-Geigy Group) to prevent degradation, after which the solvents were slowly evaporated. After complete removal of the solvent, the samples were annealed at 90 °C for 5 days.

3.2. Small angle X-ray scattering

To identify the microstructures and estimate OOT and order–disorder transition (ODT), SAXS measurements were performed on the 4C1 beamline at the Pohang Accelerator Laboratory, Korea. The X-ray wavelength was 1.608 Å. The sample was located at a distance of 2.1 m from the detector and heated at the rate of 0.5 °C/min. In order to estimate S/V, SAXS measurements were conducted with an apparatus consisting of an 18-kW rotating anode X-ray generator (Rigaku Co.) operated at 50 kV × 20 mA, mirror optics with point focusing and one-dimensional position sensitive detector (M. Braun Co.). The Cu $K\alpha$ radiation (=1.542 Å) from a 0.1 × 1 mm microfocus cathode was used. For each measurement, the sample was held at a setting temperature for 1000 s followed by data acquisition for another 4000 s. The measured intensity was corrected for background scattering and absorption by the sample. The intensity data were scaled to the absolute unit by comparison with the scattering from polystyrene [32].

The following values of specific volume were used to calculate the electron density at various temperatures [33,34]:

$$V_{PS}(PS) = 0.9217 + 5.412\times10^{-4}T + 1.687\times10^{-7}T^2 \quad (\text{above } T_g) \quad (10)$$

$$V_{PI}(PI) = 1.0771 + 7.22\times10^{-4}T + 2.46\times10^{-7}T^2 \quad (11)$$

where T is the temperature in degrees centigrade.

3.3. Rheological measurements

Using an Advanced Rheometric Expansion System (ARES, Rheometries Co.) with a 25-mm parallel plate fixture, dynamic temperature sweep experiments were performed from 85 °C to 220 °C at a heating rate of 0.5 °C/min, a frequency, ω, of 0.1 rad/s and a strain amplitude, γ_0, of 0.03, which lies in the linear viscoelastic regime under a nitrogen environment to reduce possible thermal degradation.

4. Results and discussion

Fig. 1 shows various SAXS profiles obtained from PSI0101 at different temperatures during the heating process. At

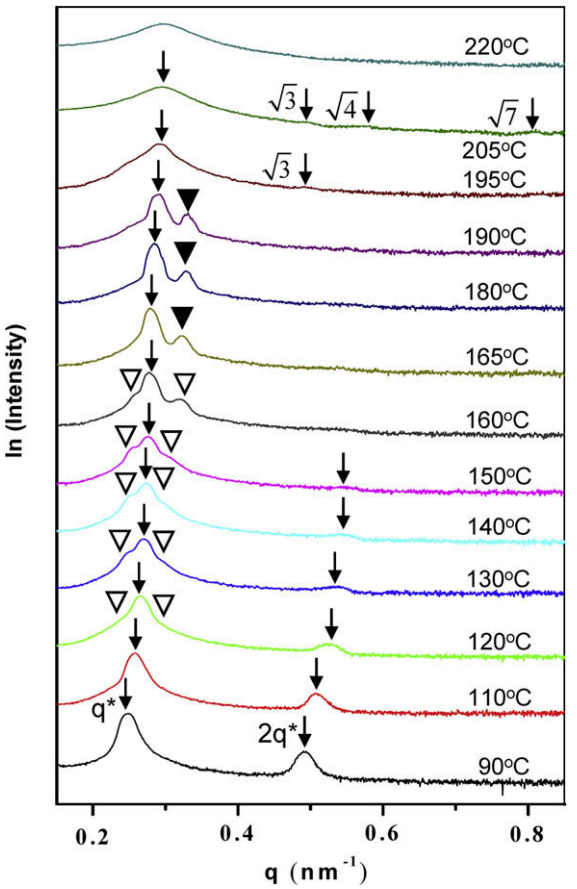

Fig. 1. SAXS profiles of PSI0101 as a function of temperature at the heating rate of 0.5 °C/min. HPL-(101) and HPL-(102) are indicated by the open triangles. G-(220) is indicated by the filled triangles.

90 °C, the specimen had an L microstructure with peaks at the relative position of q^*:$2q^*$, where q^* denotes the q value of the first-order scattering peak. The scattering profile at 110 °C showed the splitting of the first-order peak as indicated by the open triangle and arrow, which implied that the mixture was transformed from L to a new morphology. After subsequent heating to 140 °C, the SAXS pattern exhibited three peaks at the $0.92q^*$:q^*:$1.08q^*$ position, which is consistent with the scattering pattern of HPL [10,11]. At 160 °C, the first-order peak was maintained at the $0.92q^*$ position and the position of the third peak jumped from $1.08q^*$ to $1.15q^*$, which suggested the initial transformation of the HPL phase into the G phase. As temperature was increased to 165 °C, the peak at the $0.92q^*$ position disappeared and the third peak at the $1.15q^*$ position became more distinct, indicating that the transformation from HPL to G phase was completed at 165 °C. At 195 °C, the peak at the $1.15q^*$ position disappeared and the new peak at the $\sqrt{3}q^*$ position appeared. At 200 °C, the q-values marked by arrows were assigned to $1:\sqrt{3}:\sqrt{4}:\sqrt{7}$, indicating the HEX phase. Finally, at 220 °C, the SAXS profiles showed a single broad peak, indicating a disordered state. Thus, the thermally induced phase transition started in the L phase at low temperature and then sequentially moved through HPL, G and HEX phases.

Rheological measurements were performed to determine ODT and OOT. Fig. 2 shows the measured elastic modulus (G') as a function of increasing temperature. Due to the different rheological response between the microstructures, these transition behaviors induced an abrupt change in viscoelastic properties. At around 106 °C, G' did not exhibit any clear increase; nevertheless the SAXS profiles of Fig. 1 suggested an OOT from L to HPL at this temperature. The sharp increase in G' at around 152 °C indicated a second OOT from HPL to G. At around 195 °C, G' rapidly decreased over a very narrow temperature range, indicating a third OOT from G to HEX. A sharp drop of G', indicating ODT, was observed at around 214 °C. Thus, these changes in G' shown in Fig. 2 revealed the presence of four ordered phases in the sample below 214 °C. The rheological result was consistent with the OOT and ODT determinations from the SAXS patterns shown in Fig. 1.

The behaviors of the S/V ratio and interfacial thickness estimated from the scattering profiles at large q as a function of temperature can provide further information on OOT. Fig. 3 shows the results for the diblock copolymer at 90, 135, 170 and 200 °C, plotted according to Eq. (4).

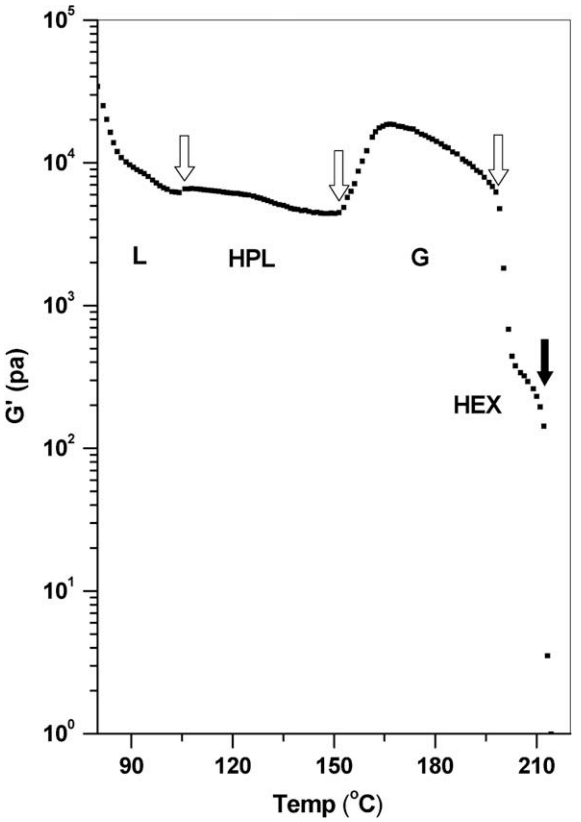

Fig. 2. Temperature dependence on heating of the dynamic shear moduli for PSI0101 at the conditions of $\omega = 0.1$ rad/s, $\gamma = 0.03$ and heating rate = 0.5 °C/min. OOTs and ODT are indicated by the open and filled arrows, respectively.

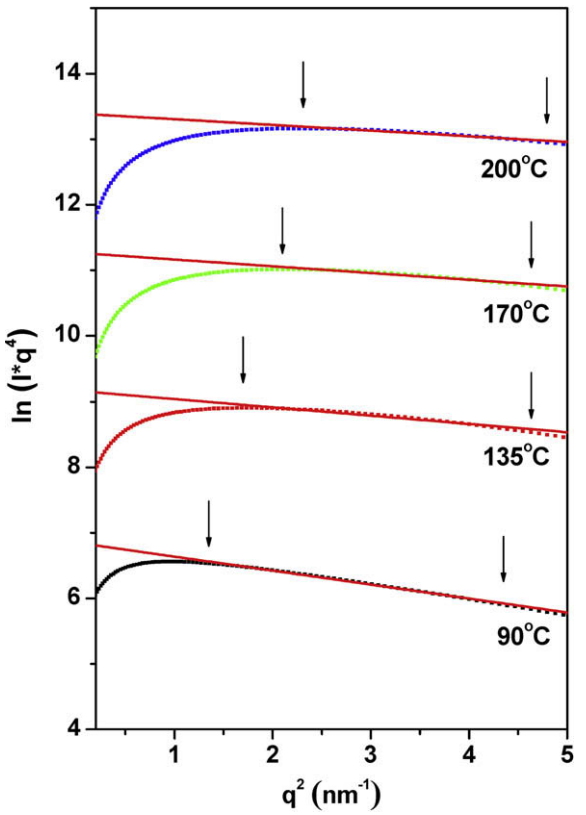

Fig. 3. The plot of $\ln(q^4 I(q))$ vs. q^2 for the diblock copolymer at 90, 135, 170 and 200 °C. This plot was constructed in order to evaluate the specific interfacial area (S/V) and interfacial thickness. For clarity only the curves obtained at 90, 135, 170 and 200 °C are plotted and the plots at 135, 170 and 200 °C are shifted upward by a factor of 2. The arrows indicate the q^2 range taken into consideration in the determination of the intercept and slope.

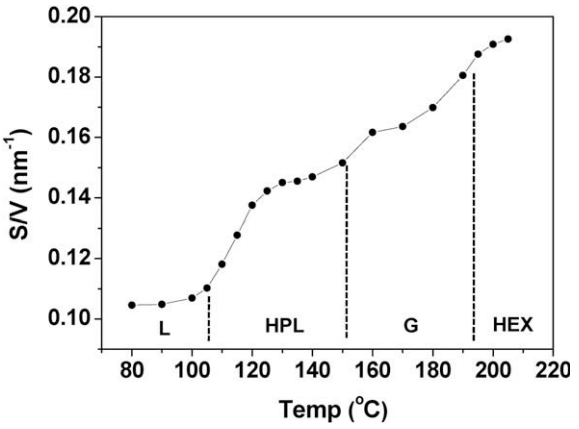

Fig. 4. The plot of specific interfacial area (S/V) as a function of temperature.

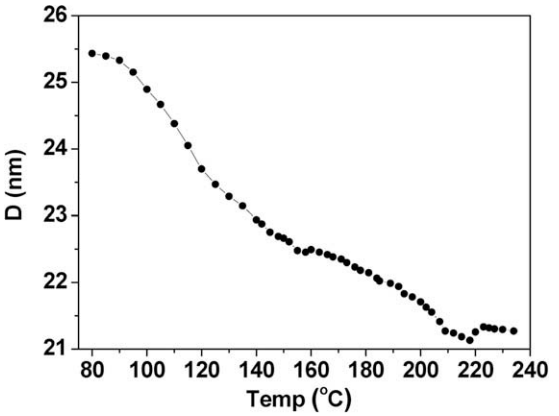

Fig. 5. The plot of the domain spacing (D) as a function of temperature.

The interfacial thickness and S/V ratio can be estimated from the slope and intercept. Before estimating S/V, interfacial thickness, and invariant, the background scattering intensity was subtracted from the observed intensity based on Eq. (6). In order to account for the statistical error of the detector, the intensity was smoothed by a suitable function. The S/V ratio gradually increased as the temperature increased from 80 °C to 105 °C (Fig. 4). In this temperature range, the SAXS pattern presented a general profile of lamellar phase (q^*:$2q^*$) and the microdomain spacing was slightly reduced from 25.4 nm to 24.7 nm (Fig. 5). As the temperature increased, the stretched polymer chains are relaxed by the increased entropy. This shrinking of chains perpendicular to the interphase leads to the decrement in the microdomain spacing and consequently, an increase in the interfacial area [35].

From 105 °C to 120 °C, the S/V ratio sharply increased, indicating an OOT from one ordered phase to another. This transition was attributed to the OOT from L to HPL indicated in the SAXS profiles of Fig. 1. From 120 °C to 140 °C, S/V was nearly constant. Fig. 5 shows the variation of domain spacing as a function of temperature. In an ideal lamellar structure, S/V can be calculated by

$$(S/V)_L = 2/D \tag{12}$$

where D is the average domain spacing of the layers. If we assume that the morphology of a diblock copolymer is the lamellar phase at 135 °C, then the two S/V ratios at 90 °C and 135 °C calculated by Eq. (11) are both 1:1.10. However, the S/V ratio obtained from the SAXS profiles between the two temperatures was 1:1.41, which was higher than the calculated ratio, indicating that another factor, other than an increase in the interfacial area by the decrement in the microdomain spacing, induced the additional S/V increase. This additional S/V increase was attributed to the contribution of the hexagonally packed channels formed by the major component material through the minor component layer.

The sharp increase of S/V from 140 °C to 160 °C and from 190 °C to 195 °C indicated the second and third OOTs from HPL to G and from G to HEX, respectively (Fig. 4). The OOTs obtained from these changes in the S/V ratios showed reasonable agreement with those determined by both the change in viscoelastic storage modulus in the rheological measurements and that in the diffraction pattern in the SAXS measurements. Matsen et al. demonstrated quantitatively that a morphological transition occurs in structures possessing more interfacial curvature [36]. The L phase

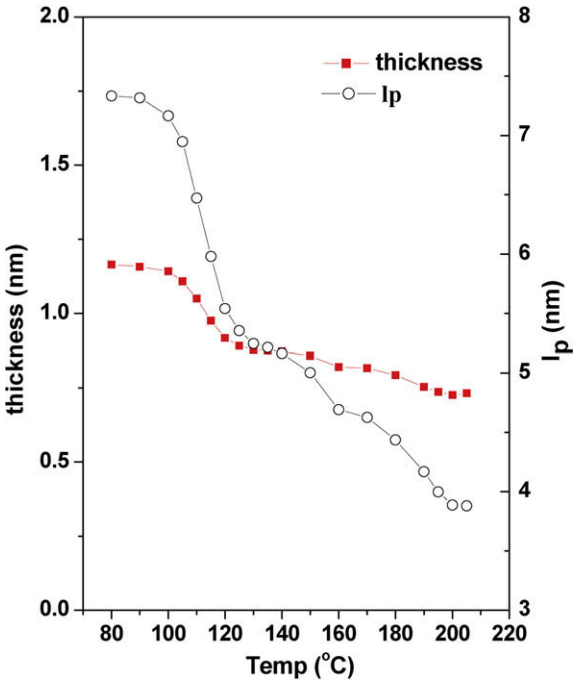

Fig. 6. The plot of interfacial thickness (■) and l_p (○) as a function of temperature.

transforms to the HEX phase through the HPL and G phases with increasing temperature because the matrix chains in HEX are less stretched than those in L, HPL and G. Therefore, the interfacial area increases because the curvature of microdomains in HEX is larger than that in L, HPL and G. Thus, the *S*/*V* ratios for L, HPL, G and HEX increase with increasing temperature, as shown in Fig. 4.

Fig. 6 presents Porod's inhomogeneity length, l_p, and the value of the interfacial thickness, *t*, as a function of temperature and as determined by Eqs. (7) and (8). The l_p value sharply decreased on the morphological transition from L to HEX through HPL and G, which was consistent with the change in the *S*/*V* ratios. The *t* value decreased sharply on the morphological transition from L to HPL. This phenomenon deserves further study.

5. Conclusion

The specific interfacial area (i.e., the *S*/*V* ratio) of the styrene–isoprene diblock copolymer showing various OOTs was estimated by analyzing the SAXS intensities in the Porod region. The *S*/*V* ratio increased gradually while Porod's inhomogeneity length, l_p, decreased sharply from L to HEX, *via* HPL and G. The interfacial thickness, *t*, on the morphological transition from L to HPL decreased sharply. The OOTs indicating a sharp increase in *S*/*V* were consistent with those determined by both the change in modulus in the rheological measurements and the diffraction pattern in the SAXS measurements.

Acknowledgements

This paper was supported by the Korea Research Foundation Grant (KRF-2007-314-D00069) and Samsung Research Fund, Sungkyunkwan University, 2008. The assistance of the Pohang Accelerator Laboratory in performing in SAXS measurements is gratefully acknowledged.

References

[1] Leibler L. Macromolecules 1980;13:1602.
[2] Bates FS, Fredrickson GH. Ann Rev Phys Chem 1990;41:525.
[3] Bates FS, Schulz MF, Khandpur AK, Förster S, Rosedale JH, Almdal K, et al. Faraday Discuss 1994;98:7.
[4] Hamley IW, Koppi KA, Rosedale JH, Bates FS, Almadal K, Mortensen K. Macromolecules 1993;26:5959.
[5] Förster S, Khandpur AK, Zhao J, Bates FS, Hamley IW, Ryan AJ, et al. Macromolecules 1994;27:6922.
[6] Hajduk DA, Harper PE, Gruner SM, Kim CC, Thomas EL, Fetters LJ. Macromolecules 1994;27:4063.
[7] Khandpur AK, Förster S, Bates FS, Zhao J, Ryan AJ, Bras W, et al. Macromolecules 1995;28:8796.
[8] Shulz MF, Khandpur AK, Bates FS, Almadal K, Mortensen K, Hajduk DA, et al. Macromolecules 1996;29:2857.
[9] Vigild ME, Almdal K, Mortensen K, Hamley IW, Faiclough JPA, Ryan AJ. Macromolecules 1998;31:5702.
[10] Ahn JH, Zin WC. Macromolecules 2000;33:641.
[11] Ahn JH, Zin WC. Macromolecules 2002;35:10238.
[12] Luo K, Yang Y. Polymer 2004;45:6745.
[13] Lambreva DM, Opitz R, Reiter G, Frederik PM, De Jeu WH. Polymer 2005;46:4868.
[14] Loo Y-L, Register RA, Adamson DH, Ryan AJ. Macromolecules 2005;38:4947.
[15] Park I, Park S, Park H-W, Chang T, Yang H, Ryu CY. Macromolecules 2006;39:315.
[16] Porod G. Kolloid – Z 1951;124:83.
[17] Porod G. Small-angle X-ray scattering. New York: Gordon & Breach; 1965.
[18] Ruland W. J Appl Crystallogr 1971;4:70.
[19] Glatter O, Kratky O. In: Small angle X-ray scattering. New York: Academic Press; 1982 [chapter 2].
[20] Roe RJ. In: Methods of X-ray and neutron scattering in polymer science. Oxford University Press; 2000 [chapter 5].
[21] Vonk CG. J Appl Crystallogr 1973;6:81.
[22] Koberstein JT, Morra B, Stein RS. J Appl Crystallogr 1980;13:34.
[23] Hashimoto T, Fujimura M, Kawai H. Macromolecules 1980;13:1660.
[24] Koberstein JT, Stein RS. J Appl Crystallogr 1983;21:2181.
[25] Roe RJ, Curro JJ. Macromolecules 1983;16:428.
[26] Zin WC, Roe RJ. Macromolecules 1984;17:183.
[27] Perrin P, Prud'shomme R. Macromolecules 1994;27:1852.
[28] Hashimoto T, Todo A, Itoi H, Kawai H. Macromolecules 1977;10:377.
[29] Todo A, Hashimoto T, Kawai H. J Appl Crystallogr 1978;11:558.
[30] Hashimoto T, Shibayama M, Kawai H. Macromolecules 1980;13:1237.
[31] Roe RJ, Chang JC, Fishkis M, Curro JJ. J Appl Crystallogr 1981;14:139.
[32] Bates FS, Rosedale JH, Bair HE, Russell TP. Macromolecules 1989;22:2557.
[33] Rigby D, Roe RJ. Macromolecules 1986;19:721.
[34] Han CD, Kim J, Kim JK. Macromolecules 1989;22:383.
[35] Hamley IW. The physics of block copolymer. New York: Oxford University Press; 1998.
[36] Matsen MW, Bates FS. Macromolecules 1996;29:7641.